Ultrahigh Vacuum Deposition of L-Cysteine on Au(110) Studied by High-Resolution X-ray Photoemission: From Early Stages of Adsorption to Molecular Organization

Grazia Gonella,[†,⊥] Silvana Terreni,[†] Dean Cvetko,[‡] Albano Cossaro,[§] Lorenzo Mattera,[†] Ornella Cavalleri,[†] Ranieri Rolandi,[†] Alberto Morgante,[§,||] Luca Floreano,[§] and Maurizio Canepa*[,†]

Dipartimento di Fisica, Università di Genova, via Dodecaneso 33, 16146 Genova, Italy, Department of Physics, University of Ljubliana, Ljubliana, Slovenia, Laboratorio INFM/TASC, Trieste, Italy, and Dipartimento di Fisica, Università di Trieste, Trieste, Italy

Received: March 25, 2005; In Final Form: July 22, 2005

We report on a high-resolution X-ray photoemission spectroscopy study on molecular-thick layers of L-cysteine deposited under ultrahigh vacuum conditions on Au(110). The analysis of core level shifts allowed us to distinguish unambiguously the states of the first-layer molecules from those of molecules belonging to the second layer. The first-layer molecules strongly interact with the metal through their sulfur headgroup. The multipeaked structure of the N 1s, O 1s, and C 1s core levels is interpreted in terms of different molecular moieties. The neutral acidic fraction ($HSCH_2CH(NH_2)COOH$) is abundant at low coverage likely associated with isolated molecules or dimers. The zwitterionic phase ($HSCH_2CH(NH_3^+)COO^-$) is largely dominant as the coverage approaches the monolayer limit and is related to the formation of ordered self-assembled molecular structures indicated by electron diffraction patterns. The occurrence of a small amount of cationic molecules ($HSCH_2CH(NH_3^+)COOH$) is also discussed. The second-layer molecules mainly display zwitterionic character and are weakly adsorbed. Mild annealing up to 100 °C leads to the desorption of the second-layer molecules leaving electronic states of the first layer unaltered.

1. Introduction

Metal surface functionalization by means of organic molecules and supramolecular architecture fabrication finds an increasing number of applications in several fields such as electronics, optics, and biotechnology.[1,2] However, the development and optimization of devices rely on a deep understanding of the physical and chemical properties of the organic/inorganic interface. The achievement of a clear picture of self-assembling processes involves the characterization of the subtle balance between molecule−molecule and molecule−surface interactions. This perspective prompted an impressive research stream on the formation of self-assembled monolayers (SAMs) on several metal substrates.[2] Organosulfur compounds deserved particular attention, and alkanethiols (ATs) deposited on Au(111), either in solution or in a vacuum, became a prototypical system.[3−5] Recently, the growing interest on bioactive surfaces is stimulating intense research on amino acids, peptides, proteins, and DNA strands.[6] SAMs of amino acids, the simplest biomolecules, received particular attention due to the possibility to address, at a reasonably manageable level of complexity, challenging issues such as the influence of multifunctionality on the assembly properties[7,8] and the chirality in two-dimensional systems.[9−10]

Among the 20 fundamental amino acids, L-cysteine, bearing a thiol headgroup, deserved particular interest as a linker of larger biomolecules[11] and chemical sensor of metal ions.[12]

A variety of ordered L-cysteine structures have been obtained on (111) gold films by means of electrochemical deposition[13−15] and self-assembly in aqueous solution.[16] Concerning deposition in ultrahigh vacuum (UHV), after pioneering work,[17] cysteine has been recently exploited to provide evidence for chiral discrimination in molecular interactions[10] and for the formation of molecular wires on the anisotropic Au(110) surface.[18] Adsorption modes on Au(111) were recently addressed by model calculations.[19,20] An adsorption configuration involving both the thiol and amino functional groups was found energetically favored at low coverage.

Our group has been recently involved in a systematic study of the adsorption of L-cysteine on gold substrates. The attention was initially placed on films deposited from high-purity solution on flame-annealed gold films displaying large, atomically flat (111) terraces. A detailed picture of the L-cysteine−Au(111) bond has been obtained by a high-resolution X-ray photoelectron spectroscopy (HR-XPS) investigation performed at the ALOISA beamline (ELETTRA).[21,22] The analysis of the S 2p core level region on pristine samples indicated the formation of a self-assembled monolayer in which all the molecules are bound to gold through their sulfur headgroup, in agreement with a secondary ions mass spectrometry study.[23] Adsorption in the disulfide form was instead discarded in agreement with calculations.[19,20] Multipeaked N 1s and C 1s spectra were rationalized in terms of the coexistence of neutral acidic ($HSCH_2CH(NH_2)COOH$) and zwitterionic ($HSCH_2CH(NH_3^+)COO^-$) moieties,[21] confirming the interpretation of early IR spectroscopy experi-

* To whom correspondence should be addressed. Fax: 0039010311066. E-mail: canepa@fisica.unige.it.
[†] Università di Genova.
[‡] University of Ljubljana.
[§] Laboratorio TASC.
[||] Università di Trieste.
[⊥] Present address: Department of Chemistry, University of Pennsylvania, Philadelphia, PA 19104-6323.

10.1021/jp051549t CCC: $30.25
Published on Web 09/01/2005

ments[24] and in substantial agreement with a recent multitechnique investigation.[25] Further, a detailed characterization of the X-ray induced damage and temperature-induced SAM alterations was carried out, showing that both irradiation and heating cause a molecular scission at the C−S bond, leaving sulfur atoms strongly bound on the surface.[21]

In this communication, we report the results of a high-resolution X-ray photoemission, HR-XPS, study of UHV deposited ultrathin films of L-cysteine on Au(110). We derive sharp criteria to distinguish the growth of the first monolayer from subsequent layer accumulation. We propose an interpretation of data in terms of different molecular moieties and suggest an interplay between such moieties and the molecular assembly. The results of this work are intended to provide a feedback for ongoing theoretical investigation[18−20] and a solid spectroscopic base for investigation of the monolayer structural properties.

2. Experimental Methods

The experiments have been performed at the ALOISA beamline of the synchrotron ELETTRA.[26]

The Au(110) substrate was prepared by 1 keV Ar^+ sputtering followed by annealing at high temperature. After this treatment, sharp (1 × 2) patterns, related to the well-known Au(110) missing row surface reconstruction, were observed in reflection high energy electron diffraction (RHEED) and grazing incidence X-ray diffraction measurements. The cleanliness of the substrate was assessed by HR-XPS surveys. No trace of sample contamination due to background gases prior to deposition was detected.

L-Cysteine (purity >99%, Sigma) was used after recrystallization in Milli-Q water.[21] Films were generally grown at room temperature. Experiments with temperatures up to 100 °C were also performed. Deposition was accomplished by a two-stage differentially pumped evaporation source[27] fitted to the ALOISA preparation chamber through a gate valve. The substrate was kept at normal incidence. L-Cysteine powder was sublimated from a boron nitride crucible. At ALOISA, the crucible to sample distance was ∼60 cm. The molecular beam was collimated through two sequential slits whose size was chosen in order to illuminate the whole sample. A working temperature of 125 °C was allowed for a deposition rate of the order of 0.1 monolayer per minute (ML/min), while keeping the background pressure in the 10^{-10} mbar range.

The HR-XPS data were obtained using a p-polarized X-ray beam at grazing incidence (about 2.5°). The spectra, taken at two typical photon energies (namely, 500 and 710 eV), were measured in normal emission by means of hemispherical electron analyzers with angular acceptance of 1°.

To control the beam damage, and taking advantage of the intense photon beam, sequential short period acquisitions on different zones of the sample were performed. A few energy windows (typically related to the O 1s, N 1s, C 1s, S 2p, Au 4f core levels, and Fermi edge region) were considered. The analyzer pass energy and acquisition times were adjusted in order to obtain a compromise among resolution, signal-to-noise ratio, and minimization of damage. An overall energy resolution of 400 and 350 meV was achieved for the spectra shown hereafter at photon energies of 710 and 500 eV, respectively. Under a typical flux density of 4×10^{10} photons/(s mm^2), the first perceptible alterations of the spectra typically occurred after about 5 min of exposure to the beam. Further details on the radiation damage can be found later on the paper and in previous reports on deposition from solution.[21,22]

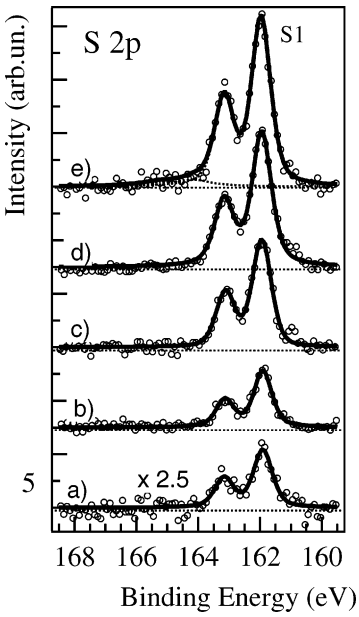

Figure 1. HR-XPS spectra obtained in the S 2p core level region as a function of coverage in the submonolayer adsorption regime, photon energy 710 eV, (a) 0.14 (b) 0.33 (c) 0.62 (d) 0.8, and (e) 1 ML. Circles: experimental data (after normalization to the photon beam flux and background subtraction). Continuous lines: best fit. Dotted lines: deconvolution with doublets of pseudo-Voigt peaks. Details on coverage calibration, background subtraction, and fitting can be found in the text.

The experimental spectra, normalized to the X-ray beam flux,[21] are reported in the next section as a function of the binding energy (BE). The BE scale was calibrated with respect to the substrate Fermi level and to the bulk Au $4f_{7/2}$ peak at 83.97 eV BE. The background due to inelastically scattered photoelectrons, calculated using the well-known Tougaard model,[28] was subtracted from raw data.

The energy position and width of XPS peaks indicated in the text were derived from multipeak fitting to pseudo-Voigt profiles.[21] The fitting curves and their subcomponents are generally represented in the figures by solid and dotted lines, respectively. S 2p doublets were fitted to pairs of peaks with the same full width at half maximum (fwhm), the standard spin−orbit splitting of 1.2 eV, and a S $2p_{3/2}$/S $2p_{1/2}$ branching ratio of 2. The position of the doublet will be conveniently identified by the position of the $2p_{3/2}$ component.

3. Results and Discussion

3.1. Room-Temperature Adsorption: First Layer Molecules. Figures 1−3 illustrate the evolution of the HR-XPS spectra (S 2p, C 1s, N 1s, and O 1s core levels) in the submonolayer regime. The S 2p region (Figure 1) is characterized by a well-defined doublet, S1. The position (161.95 ± 0.05 eV BE) and width (fwhm ∼ 0.75 eV) of S1 were constant, within experimental uncertainty, along the series of spectra. The S1 binding energy lies close to the value (161.9 ± 0.1 eV) measured for SAMs deposited from solution[21,22] and to values (∼162 eV) reported in many experiments on alkanethiols chemisorbed on gold surfaces.[29] The S1 state is accordingly assigned to the formation of a thiolate compound, after the reaction of the SH molecular termination with the substrate. Note that for the best fit of spectrum e an additional intensity (modeled through a second doublet) has been added in the 164−166 eV region. Indeed, as it is shown below, further exposure resulted in a well-defined doublet in this spectral range that,

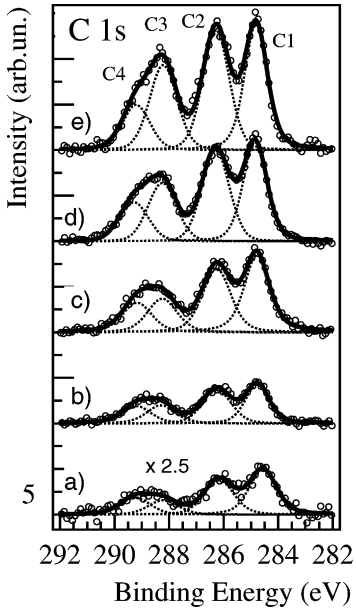

Figure 2. Same as for Figure 1 but for the C 1s core level region. Circles: experimental data (after normalization to the photon beam flux and background subtraction). Continuous lines: best fit. Dotted lines: deconvolution with pseudo-Voigt peaks.

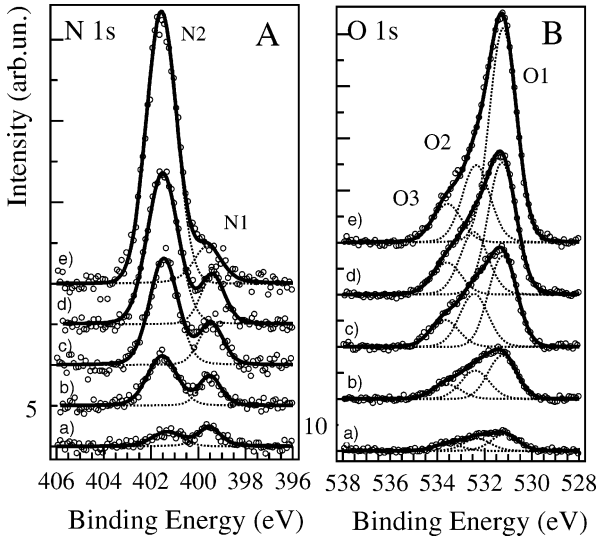

Figure 3. Same as Figures 1 and 2 but for the (A) N 1s and (B) O 1s core level regions. Circles: experimental data (after normalization to the photon beam flux and background subtraction). Continuous lines: best fit. Dotted lines: deconvolution with pseudo-Voigt peaks.

together with definite variations of the C 1s spectrum, concurred to identify the population of the second layer.

In the C 1s region (Figure 2), two well-developed peaks (C1and C2) can be identified at ∼284.7 and ∼286.2 eV BE. Although C1 is systematically higher and narrower than C2, the two peaks present a similar intensity (area). A broad structure, whose intensity is equivalent to that of C1 or C2, occurs with center of mass at ∼288.7 eV BE. Its shape evolution with coverage suggested its decomposition into two peaks. In fact, four peaks (C1, C2, C3, and C4) were necessary to reproduce the whole set of data. At the highest coverage of Figure 2, the position (fwhm) of the C1, C2, C3, and C4 peaks was determined at 284.8 ± 0.1 eV BE (1.0 eV), 286.3 ± 0.1 eV (1.2 eV), 288.2 ± 0.1 eV (1.2 eV), and 289.2 ± 0.1 eV (1.2 eV), respectively.

Following the literature on cysteine layers assembled in solution[17,21,30] and results on powders,[31] C1 and C2 can be assigned to the so-called C_β ($HSCH_2CH(NH_2)COOH$) and C_α atoms ($HSCH_2CH(NH_2)COOH$), respectively. The C3−C4 structure falls in an energy region typical of carboxyl.[17,21,30,31] Note the spectral weight change between C3 and C4 as the coverage increases.

Regarding the N 1s region (panel A in Figure 3), two relatively broad peaks were resolved, for example, N1 at 399.5 ± 0.2 eV BE and N2 at 401.5 ± 0.2 eV BE. At the lowest coverage, N1 is more intense than N2. As soon as the coverage increases N1 reaches a saturation intensity while N2 continues to increase for depositions up to 1 ML and beyond. The energy position of the N1 and N2 components in Figure 3A is found in full agreement with previous experiments on the Cys/Au system grown from the liquid phase and assigned to NH_2 and NH_3^+ groups, respectively.[17]

The O 1s spectra (panel B) exhibit a broad structure,[30,31] related to oxygen atoms belonging to COOH and COO^- groups. Its decay in the 531−530 eV region allowed us to identify with good confidence the position, intensity, and width of the lowest BE peak (O_1). The asymmetric tail toward the highest BE likely consists of a convolution of unresolved states. The whole set of data of Figure 3B was fitted with a superposition of three peaks with similar fwhm (∼1.45 eV), yielding O1 at 531.2 ± 0.1 eV, O2 at 532.3 ± 0.2 eV, and O3 at 533.6 ± 0.2 eV BE.

The coverage calibration, as reported in the figures, was derived from the analysis of the S 2p spectra.

The S1 state reaches its saturation intensity, (I^{max}_{S1}), in spectrum e. Coarse estimates of the organic layer thickness d corresponding to exposure e were obtained by exploiting the adsorbate-induced attenuation of the Au 4f line and assuming reasonable values of the electron mean free path in the organic film.[30] These estimates gave a value of $d \sim 0.5$ nm, that is compatible with the molecular dimensions,[19] and a recent determination on films deposited from solution.[30] We have therefore reasonably assumed a correspondence between I^{max}_{S1} and ∼1 ML coverage.

Further, the intensities of the C, O, and N signals (I_C, I_O, I_N) were found to depend linearly on the S 2p signal (I_S) through a proportionality constant which scales very well with the pertinent photoionization cross sections ratio. This finding added confidence about the overall integrity of adsorbed molecules and enabled us to use the $I^{(i)}_{S1}$ intensity of each measurement of Figure 1 to estimate the actual coverage $\theta^{(i)}$ through the relation $\theta^{(i)} = I^{(i)}_{S1}/I^{max}_{S1}$.

The multipeaked nature of the N 1s and O 1s levels, as well as of the carboxyl-related part of the C 1s spectrum, reflects the molecular multifunctionality.

Inspection of data (Figures 2 and 3) suggests to group peaks which exhibit a parallel evolution with coverage. The most evident "family" consists of the O1, N2, and C3 states. This combination is supported by a quantitative analysis shown in Figure 4, where the area of the peaks is reported as a function of coverage after normalization to photoionization cross section[32] σ (e.g, ${}^{\sigma}I_{Xi} = I_{Xi}/\sigma_X$) and by consideration of the molecular stoichiometry.

In Figure 4A the behavior with coverage of O1 and C3 becomes closely comparable once that half of the actual intensity of O1 (${}^{\sigma}I_{O1}/2$) is considered. At low coverage, ${}^{\sigma}I_{N2}$ values are similar to ${}^{\sigma}I_{O1}/2$ and to ${}^{\sigma}I_{C3}$. ${}^{\sigma}I_{N2}$ neatly exceeds ${}^{\sigma}I_{O1}/2$ and ${}^{\sigma}I_{C3}$ approaching the ML coverage. These findings admit the interpretation that O1, C3, and the largest part of N2 single out a well-defined chemical moiety (that we may call M_{zw}). After early experiments on cysteine films[17] and works on related

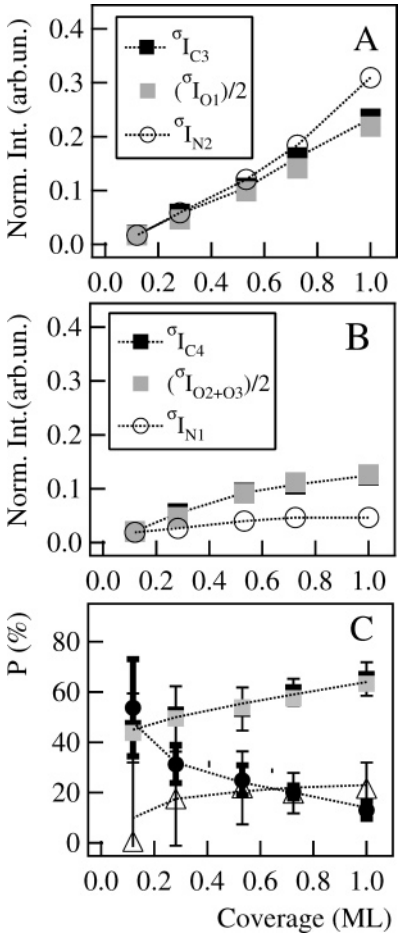

Figure 4. (A) Intensity of peaks $^{\sigma}I_{C3}$, $(^{\sigma}I_{O1})/2$, and $^{\sigma}I_{N2}$ obtained after normalization with photoionization cross sections ($^{\sigma}I_{Xi} = I_{Xi}/\sigma_X$). (B) The same for $^{\sigma}I_{C4}$, $(^{\sigma}I_{O2+O3})/2$, and $^{\sigma}I_{N1}$. (C) Relative population of zwitterionic (P_{zw}, squares) and acidic (Pac, solid circles) moieties as a function of coverage. Black and gray squares represent $P_{zw} = I_{C3}/I_{C3+C4}$ and $P_{zw} = I_{O1}/I_O$, respectively. The quantity $P_c = 1 - (P_{zw} + P_{ac})$ is also reported (triangles). Lines are guide for eyes only.

systems,[30,31,33] we assign N_2 to NH_3^+ groups. A positive BE shift of the NH_3^+-related peak with respect to the NH_2 component is expected as an effect of the electric field of a cation adjacent to the core-ionized atom.[34] A negative BE shift of the *C*OO^- carbon with respect to the *C*OOH one is expected as well.[34] Consistently with assignments of ref 21, it appears therefore reasonable to associate C3 with the carbon atom in *C*OO^- groups. In the same way, O1 could be assigned to the two equivalent oxygen atoms belonging to the so-called resonant state of the deprotonated carboxyl group.

This assignment, which refines and supersedes the one we proposed in ref 21, appears in good agreement with conclusions of literature on related systems.[8,33,35] M_{zw} can be associated to a zwitterionic phase according to such interpretation. The zwitterionic fraction P_{zw} can be determined by the I_{C3}/I_{C3+C4} intensity ratio (or, alternatively, I_{O1}/I_O).

From analysis of data it turns out that $^{\sigma}I_{C4} \sim {}^{\sigma}I_{(O2+O3)}/2$ (Figure 4B). An attractive interpretation is to put the C4 and O2−O3 states in relation to COOH groups, attributing O2 and O3 to the *O*═C−OH and O═C−*O*H states. Concerning N1 apart from the lowest coverage, it generally shows a deficit of intensity with respect to C4 and (O2 + O3)/2. Consequently, only part of C4 and O2−O3 can be associated with N1 to single out the neutral acidic phase (M_{ac}) . The percentage weight of this moiety is given by $P_{ac} = I_{N1}/I_N$.

The part of N2 which has not been associated with M_{zw} (e.g., $I_{N2}/I_N - P_{zw}$) and the part of the C4 and O2−O3 states which have not been related with M_{ac} (e.g., $I_{C4}/I_{C3+C4} - P_{ac}$ or $I_{O2+O3}/I_O - P_{ac}$) must belong to other moieties (M_c), with weight given by the relation $P_c = 1 - (P_{zw} + P_{ac})$. P_{ac}, P_{zw}, and P_c are reported in Figure 4C as a function of coverage. We remark the good agreement between zwitterionic fractions calculated starting from carbon and oxygen peaks, respectively. At low coverage, P_{zw} and P_{ac} form almost the totality of the population; at monolayer saturation, $P_{zw} + P_{ac} \sim 80\%$ and $P_c \sim 20\%$.

It could be simple to identify M_c with cationic species ($HSCH_2CH(NH_3^+)COOH$). In this respect, several mechanisms of proton trapping, originating from the S−H bond breaking or from beam damage, can be speculated, especially in the case of a compact monolayer. However, the value of P_c at monolayer saturation, if interpreted in terms of cationic species exclusively, should involve an unexpected amount of surface charge.

It must be noted that in the absence of an unambiguous evidence of satellite features we considered initial state arguments only. However, taking into account the current description of the Cys/Au valence band,[19] HOMO−LUMO shake-up features could potentially affect the high BE tails of the carboxyl and oxygen peaks (C4 and/or O2 + O3). Ignoring these contributions leads to underestimate P_{zw} and, therefore, to overestimate P_c.

Further, we have to remark that in our analysis we neglected the adsorption configuration. The reciprocal position of emitters potentially affects the angle resolved detected intensity through "shadowing" effects and differential attenuation and even diffraction/focusing effects in the trajectory of photoelectrons. Different adsorption geometries for zwitterionic and acidic molecules, which are conceivable in view of recent scanning tunnel microscopy (STM) studies[10,18] and possibly depending on molecular packing conditions, might perturb the determination of P_{zw}, P_{ac}, and consequently, P_c. In particular, if such effects were responsible, at least in part, for the excess of $^{\sigma}I_{N2}$ toward monolayer saturation in Figure 4A, then $P_{ac} = I_{N1}/I_N$ would exceed the estimate reported in Figure 4C.

Therefore, the value reported in Figure 4C likely represents only an upper limit for P_c. The actual population of cationic molecules should deserve further investigation with other spectroscopic methods.

We will now concentrate the discussion on the coverage evolution of P_{zw} and P_{ac}, at very low coverage $P_{ac}-P_{zw}$. Figure 4C as well as the saturation behavior of N1 in Figure 3A (and 4B) indicate that the neutral acidic phase is characteristic of the initial stage of adsorption. The P_{ac} fraction may be assigned to isolated molecules, eventually bound to surface defects. Further, P_{ac} could be associated with randomly distributed dimers nucleated across the added rows, as observed in STM pictures at low coverage.[10,18] Such dimers have been claimed to be formed by neutral molecules, interacting with the substrate through their S terminations and the amino groups, and linked by double hydrogen bonds between carboxyl groups.[10]

As soon as the coverage increases, the M_{zw} becomes by far the leading phase. This conclusion appears in substantial agreement with findings of ref 25 (on Au(111)), where an exclusively zwitterionic layer was characterized by ion scattering techniques and with results obtained for deposition from the liquid phase on gold (111) films[21] and on related systems.[35]

We note that at submonolayer coverage, RHEED surveys and preliminary GIXRD results show the occurrence of relatively sharp (1 × 4) patterns which quality improves with mild annealing (up to 100 °C) or for deposition at temperatures higher

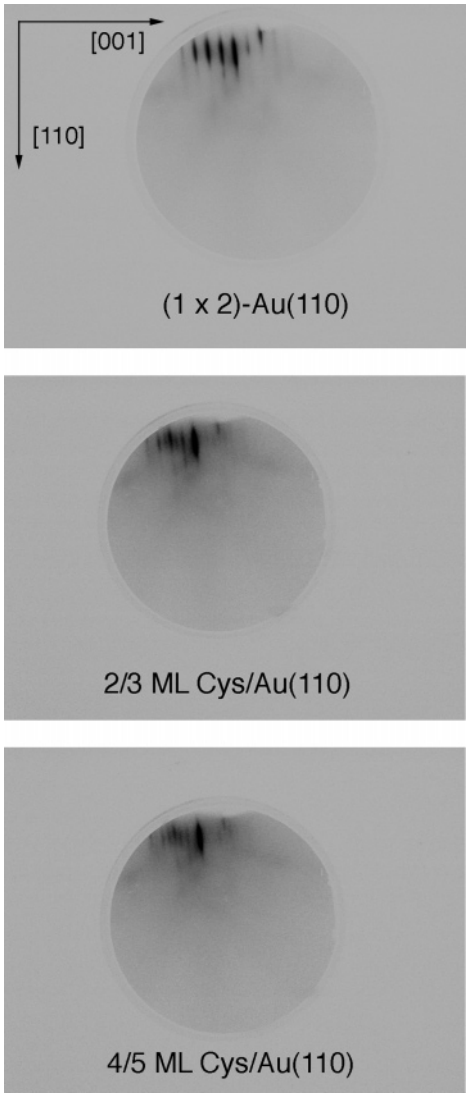

Figure 5. RHEED patterns obtained at various stages of deposition at 60 °C. The coverage was calibrated by photoemission spectra according to the procedure described in the text. Upper panel: (1 × 2) pattern obtained on the bare substrate. Central panel: 0.66 ML of cysteine. Lower panel: 0.8 ML of cysteine. The patterns have been detected under a short exposure to the electron beam and a low beam intensity to minimize layer damage.

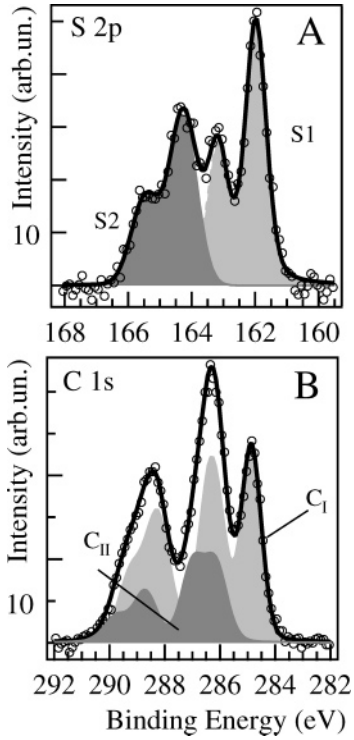

Figure 6. HR-XPS spectra obtained after saturation of the first layer, photon energy 500 eV, (A) S 2p, (B) C 1s. Circles: background subtracted experimental data. Continuous lines: fit. Light gray: spectral component originating from first-layer molecules. Gray: spectral component originating from second-layer molecules. Mild annealing up to 100 °C produce spectra which are practically a replica of the light gray components.

than room temperature. Representative RHEED images are reported in Figure 5.

Fourth-integer spots appear in RHEED images at about 0.5 ML. A well-defined (1 × 4) pattern is developed before the completion of the first monolayer (Figure 5). At the same time, the integer and half-integer peaks arising from the substrate missing row reconstruction start fading, without apparent broadening. These findings generally suggest a change of the substrate reconstruction into a smoother interface. They also suggest that the substrate missing row reconstruction drives some kinds of anisotropic growth as observed for other molecules.[36,37]

We assign P_{zw} to the molecules yielding the long-range ordered structure which is reflected in the (1 × 4) symmetry RHEED patterns. In this respect, our diffraction patterns appear to be correlated with the results of recent scanning probe investigations where long molecular chains, extending along the [110] direction and paired into coupled rows in the [001] direction, have been reported.[18] Indeed, the high-resolution pictures of ref 18 put forward a sort of "zigzag" connection between two rows of molecules which could figure a network-like structure, not much dissimilar, in its essential character, from those found in other STM investigations on (111) samples.[13−15]

If the molecular structure of cysteine is considered,[19] the zwitterionic fraction of the first-layer molecule seems compatible with the formation of these networks, possibly representing a precursor stage to peptide bond formation.

From this discussion it looks conceivable that the amount of zwitterionic vs the acidic fraction is dependent on the lattice symmetry of the metal surface. The amount of defects of the particular samples involved in the measurements could be an important parameter as well. Further experiments to elucidate these points would be desirable.

We conclude this section by mentioning that mild annealing, up to 100 °C, did not involve significant changes of the first monolayer XPS spectra. Only a slight narrowing of the S1 state is observed which can be correlated with ordering effects.

3.2. Beyond the Monolayer. The population of the second layer was identified by analysis of S 2p and C 1s core levels. Figure 6 deals with films of thickness exceeding that of Figure 1. Data were obtained with 500 eV photons. The S 2p spectrum (upper panel) could be fitted with two doublets. S1 (light gray) exhibits the same position, width, and a slight attenuation of intensity found, under the same experimental conditions, at 1 ML. A second doublet (S2) can be observed at 164.3 ± 0.1 eV BE. Its fwhm turns out to be 1.05 eV vs 0.8 eV found for S1.

The binding energy of S2 is in good agreement with early low-resolution experiments where it was assigned to a "dangling"-SH termination.[17] Further, a peak of similar BE was found for "unbound" sulfur in cysteine-containing peptides immobilized on a gold surface.[38] Therefore, the association of S2 with intact

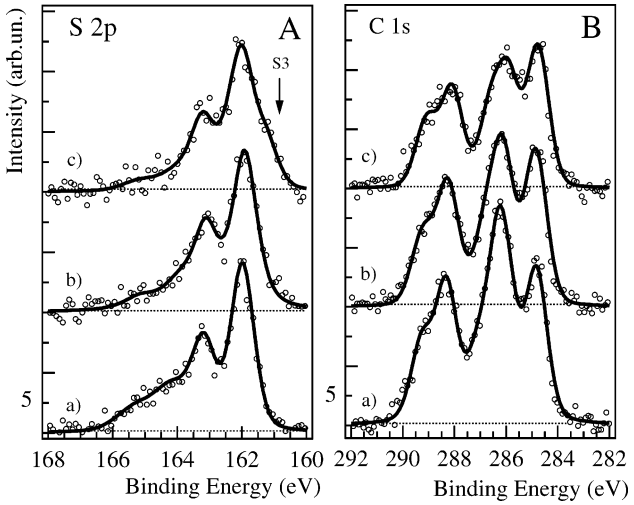

Figure 7. HR-XPS spectra obtained as a function of irradiation time, on films with initial second-layer population, photon energy 700 eV, (A) S 2p, (B) C1s. Typical flux density: 4×10^{10} photons/(s mm^2). Irradiation time: (a) 5 min, (b) $^1/_2$ h, (c) 2 h. Circles: background subtracted experimental data. Continuous thick lines are a guide for the eyes. S3 indicates a S 2p state originating from an irradiation-induced scission of intramolecular bonds.[22]

molecules, softly landed on the first layer, seems both easy and attractive. In this view, the broadening of S2 (with respect to S1) can be due to disorder in the second layer.

Dimerization through −S−S− bonds to form cysteine molecules should be taken into account as well. However, the S2 binding energy appears significantly larger than the values reported in the literature for both sulfide and disulfide moieties (generally found in the range 163−163.5 eV BE[39]).

In Figure 6B, the C 1s spectrum can be compared with the fit to data obtained (with the same photon energy) at 1 ML (light gray). The differences suggest the occurrence of a shifted set of "second-layer" states. Further support to this interpretation scheme could be inferred by experiments performed as a function of the irradiation time and as a function of the annealing temperature.

In Figure 7A, the comparison of spectra a and b shows a "fast" removal of S2. The much slower decrease of S1 is accompanied by the growth of a third state at ∼161.2 eV (S3), associated with molecular fragmentation.[21,22] A neat decrease of intensity of the prominent structure at ∼286.2 eV is observed in the corresponding C 1s spectra (panel 7B).

These findings illustrate the X-ray induced sputtering of second-layer molecules. On the other hand, mild annealing (80−100 °C) of films presenting second-layer population (as well as of multilayers) resulted in spectra closely similar to the light gray parts of Figure 6 apart from minute intensity changes related to attenuation of first-layer features due to second-layer molecules.

These findings demonstrate the temperature-induced desorption of weakly bound molecules, in excellent agreement with results obtained on Au(111),[25] where desorption of cysteine multilayers is reported at 353−373 K in a mass spectrometry thermal programmed desorption experiment. Indeed, we could obtain single monolayer spectra through overdosing L-cysteine at a substrate temperature of 100 °C.

Coming back to the data in Figure 6B it has become clear that the peak at the lowest BE is related to first-layer molecules only. The huge peak at ∼286.5 eV and the carboxyl region are instead a superposition of first-layer and second-layer features. We attempted to fit the data to a superposition of the " first-layer" profile (C_I) and several peaks (with the same width) forming the profile due to second-layer molecules (C_{II}). These assumptions appear fully justified regarding the first-layer C1 and C2 peaks, whose features, as is evident from Figure 1, seem tightly correlated. They are somewhat weak regarding the carboxyl-related region, where a strong correlation is expected between first- and second-layer features. The fit required four "second-layer" peaks. Two peaks found at 286.1 eV (C1′) and 287 eV (C2′) were assigned to the C_β and C_α states of second-layer molecules, respectively. Note that the $C_\beta-C_\alpha$ energy separation (0.9 eV) is smaller than that in the first-layer molecules (1.5 eV) approaching the calculated value (0.7 eV) for the free molecule.[40]

Two other peaks were found in the carboxyl region at 288.7 eV (C3′) and 289.7 (C4′) eV. Considering initial state effects only, C3′ and C4′ should be tentatively assigned to COO^- and COOH groups. Indeed, N 1s and O 1s spectra taken at a coverage approximately corresponding to the situation depicted in Figure 6 (not shown) continue the trend illustrated in Figure 3. In particular, second-layer molecules add intensity to the NH_3^+-related peak at 401.5 eV BE, which largely prevails over the NH_2 one. Such findings would imply that second-layer molecules are mainly zwitterionic but with a large and unexpected fraction of cations. We believe that these findings reinforce the hypothesis that the carboxyl-related part of the C 1s spectra is affected by significant shake-up contributions, leading to a sizable overestimation of the cationic fraction.

Conclusions

We have reported and discussed high-resolution X-ray photoemission spectroscopy measurements on molecular-thick films of L-cysteine deposited at room temperature under ultrahigh vacuum conditions on a Au(110) surface. The analysis of core level shifts allowed us to disentangle first-layer molecules, strongly interacting with the metal, from weakly adsorbed second-layer molecules. The N 1s, O 1s, and C 1s core levels present a multipeaked structure depicting a rich scenario of chemical states. The neutral acidic fraction ($HSCH_2$-$CH(NH_2)COOH$) is relevant only at low coverage, likely related to isolated molecules or to the dimers observed in recent STM experiments, and possibly related to the surface morphology of the substrate (regarding both the defect density and its typical reconstruction). The population weight of the zwitterionic ($HSCH_2CH(NH_3^+)COO^-$) fraction increases to become the main one as coverage approaches the monolayer limit and beyond. The possible occurrence of molecules with cationic character ($HSCH_2CH(NH_3^+)COOH$) at the submonolayer level has been also discussed.

We proposed to put the zwitterionic molecules in the first monolayer in connection to the formation of self-assembled molecular networks yielding a (1×4) symmetry in RHEED patterns. We hope that the conclusions of this paper could prompt further theoretical effort for the inclusion of zwitterions in the calculation of the SAM electronic structure and geometry.

Acknowledgment. This project has been co-financed by the University of Genova and MIUR (PRIN Project 2003028141_005). Financial support by the FIRB ''Molecular Nano-Devices" project and INFM (PURS project) is also acknowledged. Paolo Pelori and Antonio Gussoni are warmly acknowledged for their support in the design and realization of the deposition system. M.C. thanks Salvatore Iannotta for fruitful discussion on the design of the source and Francesco Bisio for a critical reading of the manuscript.

References and Notes

(1) Kasemo, B. *Surf. Sci.* **2002**, *500*, 656.
(2) Ulman, A. *Chem. Rev.* **1996**, *96*, 1533.
(3) Schreiber, F. *Prog. Surf. Sci.* **2000**, *65*, 151.
(4) Chidsey, C. E. D.; Liu, G.-Y; Rowntree, P.; Scoles, G. *J. Chem. Phys.* **1989**, *91*, 4421.
(5) Nuzzo, R. G.; Dubois, L. H.; Allara, D. L. *J. Am. Chem. Soc.* **1990**, *112*, 2, 558.
(6) Lindroos, K.; Liljedahl, U.; Raitio, M.; Syvänen, A. C. *Nucleic Acids Res.* **2001**, *29*, e69.
(7) Barlow, S. M.; Raval, R. *Surf. Sci. Rep.* **2003**, *50*, 201.
(8) Zubavichus, Y.; Zharnikov, M.; Yang, Y.; Fuchs, O.; Heske, C.; Umbach, E.; Tzvetkov, G.; Netzer, F. P.; Grunze, M. *J. Phys. Chem. B* **2005**, *109*, 884.
(9) Atanasoska, L. L.; Buchholz, J. C.; Somorjai, G. A. *Surf. Sci.* **1978**, *72*, 189.
(10) Kühnle, A.; Linderoth, T. R.; Hammer, B.; Besenbacher, F. *Nature* **2002**, *415*, 891.
(11) Chi, Q.; Zhang, J.; Nielsen, J. U.; Friis, E. P.; Chorkendorff, I.; Canters, W. G.; Andersen, J. E. T.; Ulstrup, J. *J. Am. Chem. Soc.* **2000**, *122*, 4047.
(12) Liu, A.-C.; Chen, -C.; Lin, C.-C.; Chou, H.-H.; Chen, C.-H. *Anal. Chem.* **1999,** *71*, 1549.
(13) Dakkouri, A. S.; Kolb, D. M.; Edelstein-Shima, R.; Mandler, D. *Langmuir* **1996**, *12*, 2849.
(14) Zhang, J.; Chi, Q.; Nielsen, J. U.; Friis, E. P.; Andersen, J. E. T.; Ulstrup, J. *Langmuir* **2000**, *16*, 7229.
(15) Xu, Q.-M.; Wan, L.-J.; Wang, C.; Bai, C.-L.; Wang, Z.-Y.; Nozawa, T. *Langmuir* **2001**, *17*, 6203.
(16) Dodero, G.; De Micheli, L.; Cavalleri, O.; Rolandi, R.; Oliveri, L.; Daccà, A.; Parodi, R. *Colloids Surf.* **2000** , *175*, 121.
(17) Uvdal, K.; Bodö, P.; Liedberg, B. J. *Colloid Interface Sci.* **1992**, *149*, 162.
(18) Kühnle, A.; Molina, L. M.; Linderoth, T. R.; Hammer, B.; Besenbacher, F. *Phys. Rev. Lett.* **2004**, *93*, 086101.
(19) Di Felice, R.; Selloni, A.; Molinari, E. *J. Phys. Chem. B* **2003**, *107*, 1151.
(20) Di Felice R.; Selloni, A. *J. Chem. Phys.* **2004**, *120*, 4906.
(21) Cavalleri, O.; Gonella, G.; Terreni, S.; Vignolo, M.; Floreano, L.; Morgante, A.; Canepa, M.; Rolandi, R. *Phys. Chem. Chem. Phys.* **2004**, *6*, 4042.
(22) Cavalleri, O.; Gonella, G.; Terreni, S.; Vignolo, M.; Pelori, P.; Floreano, L.; Morgante, A.; Canepa, M.; Rolandi. *J. Phys.: Condens. Matter* **2004**, *16*, S2477.
(23) Leggett, G. J.; Davies, M. C.; Jackson D. E.; Tendler, J. B. *J. Phys. Chem.* **1993**, *97*, 5348.
(24) His, A.; Liedberg, B. *Colloid Interface Sci.* **1991**, *144*, 282. (b) Uvdal, K.; Vikinge, T. P. *Langmuir* **2001**, *17*, 2008;
(25) Shin, T.; Kim, K.-N.; Lee, C.-W.; Shin, S. K.; Kang, H. *J. Phys. Chem. B* **2003**, *107*, 11674.
(26) Gotter, R.; Ruocco, A.; Morgante, A.; Cvetko, D.; Floreano, L.; Tommasini, F.; Stefani, G. *Nucl. Instrum. Methods Phys. Res., Sect. A* **2001**, *1468*, 467. (b) Floreano, L.; Naletto, G.; Cvetko, D.; Gotter, R.; Malvezzi, M.; Marassi, L.; Morgante, A.; Santaniello, A.; Verdini, A.; Tommasini, F.; Tondello, G. *Rev. Sci. Instrum.* **1999** , *70*, 3855.
(27) Pelori, P. Laurea Thesis, University of Genova, 2004 (in Italian), available on request in electronic format.
(28) Tougaard, S. *Surf. Sci.* **1989**, *216*, 343.
(29) Laibinis, P.; Bain, C.; Whitesides, G. *J. Phys. Chem.* **1991**, *95*, 7017.
(30) Beerbom, M. M.; Gargagliano, R.; Schlaf, R. *Langmuir* **2005**, *21*, 3551.
(31) Brizzolara, R. A. *Surf. Sci. Spectra* **1997**, *4*, 102.
(32) Cross sections from http://ulisse.elettra.trieste.it/services/elements.
(33) Löfgren, P.; Krozer, A.; Lausmaa, J.; Kasemo, B. *Surf. Sci.* **1999**, *370*, 277.
(34) Bagus, P. S.; Illas, F.; Pacchioni, G.; Parmigiani, F. *J. Electron Spectrosc.Relat. Phenom.* **1999**, *100*, 215.
(35) Mateo Marti, E.; Methivier, Ch.; Pradier, C. M. *Langmuir* **2004**, *20*, 10223.
(36) Cossaro, A.; Cvetko, G.; Bavdek, L.; Floreano, R.; Gotter, A.; Morgante, F.; Evangelista, A.; Ruocco, J. *Phys. Chem. B* **2004**, *108*, 14671.
(37) Prato, S.; Floreano, L.; Cvetko, D.; De Renzi, V.; Morgante, A.; Modesti, S.; Taliani, C.; Zamboni, R.; Biscarini, F. *J. Phys. Chem.* **1999**, *103*, 7788.
(38) Bass, T.; Gamble, L.; Hauch, K. D.; Castner, D. G.; Sasaki, T. *Langmuir* **2002** , *18*, 4898.
(39) Heister, K.; Zharnikov, M.; Grunze, M.; Johansson, L. S. Q.; Ulman, A. *Langmuir* **2001**, *17*, 8.
(40) Plashkevych, O.; Carravetta, V.; Vahtras, O.; Ågren, H. *Chem. Phys.* **1998**, *232*, 49.